Hindawi
Mathematical Problems in Engineering
Volume 2020, Article ID 8891046, 9 pages
https://doi.org/10.1155/2020/8891046

*Research Article*

# Model-Based Stochastic Adaptive Air-Fuel Ratio Control of Direct Injection Biogas-Fuelled Engines

**Jun Yang, Yanxiao Li, Jian Wang, and Fangyuan Li**

*Department of Automotive Engineering, Shandong Jiaotong University, Jinan 250357, China*

Correspondence should be addressed to Jun Yang; yang222401@163.com

Received 13 September 2020; Revised 31 October 2020; Accepted 5 November 2020; Published 19 November 2020

Academic Editor: Kauko Leiviskä



The problem of stochastic adaptive air-fuel ratio control by the dynamic model of biogas-fuelled engines is investigated in this paper. An adaptive law is employed to estimate the theoretical air-fuel ratio, which is undetermined due to the uncertainty of the methane concentration in the biogas. A stochastic adaptive air-fuel ratio controller in consideration of the stochasticity of the residual gas is designed based on the adaptive law, and the closed-loop system is proven to be mean-square stable. The proposed stochastic adaptive air-fuel ratio controller is validated through a numerical simulation when the theoretical air-fuel ratio is unknown constants and jump signals.

## 1. Introduction

As a promising alternative energy, biogas has been applied to the internal combustion engines to decrease emissions and fuel consumption. The methane concentration which indicates the thermal value of the biogas varies in a certain range [1]. The uncertainty of the methane concentration greatly affects the performance of the engines, and the corresponding problems have received much attention.

The effect of the chamber form of combustion, advance of ignition timing, and ratio of compression to the biogas-fuelled engine, which is modified from the diesel engine through simulation, was investigated in [2], and the optimal advance of ignition timing was determined by the methane concentration of the biogas and engine revolution. Three kinds of biogas with different methane concentrations were used to experimentally study the effect of the biogas composition on the performance, emissions, and combustion of the compression ignition biogas diesel engine with the characteristic of premixed charge in [3]. The influence from the components of the biogas to the characteristics of emission and performance of a dual fuelled compression ignition miniature engine was deduced in [4] by using biogas with three different levels of methane concentrations, and the analyzation of exergy was provided to discover the inefficiencies of each process. The biogas with sixty percent methane was used to investigate the effect from the biogas to the thermal barrier-coated engine with a dual-fuel system by the experimental method in [5] in order to achieve the decrease of smoke emissions. The effect of the variation of the methane concentration in biogas to the conversion efficiency of the energy and emissions of the engine with characteristics of dual fuel and common rail was discussed in [6], and the effect from the pilot and postspray of diesel was considered. The methane energy was used to supplement the diesel power in a certain percentage in [7] to release the relationship between the increase in methane and the emissions and performance of a dual-fuelled engine. Biogas with two different methane concentrations was applied to evaluate the emissions and performance of a miniature biogas-fuelled Otto cycle engine with one cylinder in [8] with consideration of the ratio of compression and crown geometry of the piston.

However, research results on the effect of the uncertainty of the methane concentration on the control accuracy of the air-fuel ratio have rarely been reported. The control accuracy of the air-fuel ratio directly affects the emissions and fuel consumption of the biogas-fuelled engines. Indeed, the uncertainty of the methane concentration results in the

undetermined theoretical air-fuel ratio, which together with the stochasticity of the residual gas makes the air-fuel ratio control inaccurate. An applicable method to overcome this problem is to design a stochastic adaptive controller, by which the theoretical air-fuel ratio can be estimated, and the stochasticity of the residual gas can be attenuated. In fact, the stochastic and/or adaptive control algorithm has been widely studied and applied to many practical systems. The fuzzy adaptive tracking controller for the indeterminate switched nonlinear system with pure feedback and nonlinear characteristics in consideration of immeasurable states was designed by Ma et al. [9], and the stability was deduced in the finite-time sense. The output feedback fuzzy adaptive tracking control problem for stochastic switched systems with pure feedback and nonlinear characteristics in consideration of nonlinear uncertain functions and immeasurable states was investigated in [10]. By considering the indeterminate switched system, dynamics of unmodeled parts, saturation of input, output with unknown dead zone, disturbances of dynamic, and immeasurable states, the fuzzy adaptive tracking controller for the unsure switched system with nonlinear characteristics was provided in [11]. The output feedback fuzzy $H_\infty$ controller for systems with discrete-time and nonlinear characteristics considering the uncertain protocol of communication and quantization was designed in [12]. Based on an adaptive reference algorithm of the state of charge, a model predictive controller, which is based on the Markov chain, was designed for the minimum consumption of energy and high efficiency of the algorithm of the electric plug-in hybrid passenger car in [13], and many key factors that significantly affect the efficiency of computation were studied. A unique stochastic adaptive model predictive controller, which contains the probability calculated framework of cut in, was designed in [14] to improve the reaction precision to the danger from the detected cut-in maneuver, which is crucial for the performance enhancement of the system of adaptive cooperative cruise control. An adaptive stochastic control algorithm, which contains the superiorities of the certain control algorithm, was investigated in [15] to improve the control performance of the stochastic control algorithm to limit the engine knock, and the proposed control algorithm was validated by numerical simulation and experiment. A stochastic adaptive model predictive controller for the electric hybrid plug-in bus was proposed in [16] based on a stochastic model of driving with Markov characteristic, and a function of piecewise was used to regulate the parameters to achieve the tradeoff between the economy of fuel and vehicle following in the given cost function. The resilient state feedback control algorithm of an intelligent automobile to regulate the lateral movement considering the stochastic-produced uncertainties was designed in [17].

The stochastic adaptive control algorithm is applied to the air-fuel ratio control problem of the biogas-fuelled engines in this paper to decrease emissions and fuel consumption, and the closed-loop system is proven to be mean-square stable. The effectiveness of the proposed stochastic adaptive controller is verified by the numerical simulation from which we can observe that the proposed stochastic adaptive controller has preferred control performance.

## 2. Controller Design

The design process of the stochastic adaptive air-fuel ratio controller is provided in this section. The discrete-time dynamic model in [18] is used to describe the dynamics of the air path and fuel path of the direct injection biogas-fuelled engines:

$$\begin{aligned} M_a(k+1) &= \left(M_a(k) - \lambda_d \mu M_f(k)\right) r(k) + M_{\text{an}}(k) \\ &\quad + \Delta M_{\text{an}}(k), \\ M_f(k+1) &= M_f(k)(1-\mu) r(k) + M_{\text{fn}}(k), \end{aligned} \tag{1}$$

where $M_a(k)$ and $M_f(k)$ mean the masses of total air and total fuel at the beginning of the combustion stroke, $\lambda_d$ means the theoretical air-fuel ratio, $\mu \in (0,1)$ means the combustion efficiency, $r(k)$ means the residual gas fraction, $M_{\text{an}}(k)$ means the mass of fresh air, $M_{\text{fn}}(k)$ means the mass of fresh fuel, and $\Delta M_{\text{an}}(k)$ means the fluctuation of the mass of fresh air and can be considered a Gaussian white noise. We define the regulation error of the air-fuel ratio $y(k)$ as

$$y(k) = M_a(k) - \lambda_d M_f(k). \tag{2}$$

Substituting (1) into (2), we get

$$y(k+1) = r(k) y(k) + M_{\text{an}}(k) - \lambda_d M_{\text{fn}}(k) + \Delta M_{\text{an}}(k). \tag{3}$$

The deterministic part of system (3) is used to design the stochastic adaptive air-fuel ratio controller:

$$y(k+1) = r(k) y(k) + M_{\text{an}}(k) - \lambda_d M_{\text{fn}}(k). \tag{4}$$

In the design process of the stochastic adaptive air-fuel ratio controller, the theoretical air-fuel ratio $\lambda_d$ is considered as an unknown constant, and residual gas fraction $r(k)$ is modeled as a finite-state, irreducible, aperiodic Markov chain with value set $S = \{s_1, s_2, \ldots, s_N\}$ and one-step transition probability $p_{s_i s_j}$. The theoretical air-fuel ratio $\lambda_d$ is estimated by an adaptive law, which is deduced by [19]

$$\widehat{\lambda}_d(k+1) = \widehat{\lambda}_d(k) + c\left(y(k+1) - \widehat{y}(k+1)\right), \tag{5}$$

where $\widehat{\lambda}_d(k)$ means the estimation of $\lambda_d$ at the $k$-th cycle, $c$ is a design parameter, and $\widehat{y}(k)$ means the estimation of $y(k)$, which is obtained by $\widehat{\lambda}_d(k)$ as follows:

$$\widehat{y}(k+1) = r(k) y(k) + M_{\text{an}}(k) - \widehat{\lambda}_d M_{\text{fn}}(k). \tag{6}$$

With (4)–(6), we have

$$\widehat{\lambda}_d(k+1) = \widehat{\lambda}_d(k) - c M_{\text{fn}}(k) \widetilde{\lambda}_d(k), \tag{7}$$

where

$$\widetilde{\lambda}_d(k) = \lambda_d - \widehat{\lambda}_d(k). \tag{8}$$

For system (4), we select a Lyapunov function as

$$V(k, r(k) = s_i) = \varepsilon(s_i) y^2(k) + \tilde{\lambda}_d^2(k), \tag{9}$$

where $\varepsilon(s_i) > 0$ is a design parameter. Based on (4), (7), and (8), the difference of (9) can be calculated as

$$\begin{aligned}\Delta V(k, r(k) = s_i) &= E[V(k+1, r(k+1)) | r(k) = s_i] - V(k, r(k) = s_i) \\ &= E[\varepsilon(r(k+1)) | r(k) = s_i] y^2(k+1) + \tilde{\lambda}_d^2(k+1) - \varepsilon(s_i) y^2(k) - \tilde{\lambda}_d^2(k) \\ &= \sum_{j=1}^{N} p_{s_i s_j} \varepsilon(s_j) (r(k) y(k) + M_{\text{an}}(k) - \lambda_d M_{\text{fn}}(k))^2 \\ &\quad + (\tilde{\lambda}_d(k) + c M_{\text{fn}}(k) \tilde{\lambda}_d(k))^2 - \varepsilon(s_i) y^2(k) - \tilde{\lambda}_d^2(k).\end{aligned} \tag{10}$$

By setting the mass of the fresh fuel $M_{\text{fn}}(k)$ to be

$$M_{\text{fn}}(k) = \frac{r(k) y(k) + M_{\text{an}}(k)}{\hat{\lambda}_d(k)}, \tag{11}$$

when design parameters $c$ and $\varepsilon(s_i)$ satisfy

$$\begin{aligned} c &= -\frac{1}{\sup\{M_{\text{fn}}(k)\}}, \\ \varepsilon(s_i) &= \frac{1}{(\sup\{M_{\text{fn}}(k)\})^2}, \end{aligned} \tag{12}$$

we obtain

$$\begin{aligned}\Delta V(k) &= V(k+1) - V(k) \\ &= \sum_{j=1}^{N} p_{s_i s_j} \varepsilon(s_j) M_{\text{fn}}^2(k) \tilde{\lambda}_d^2(k) + (1 - c M_{\text{fn}}(k))^2 \tilde{\lambda}_d^2(k) - \varepsilon(s_i) y^2(k) - \tilde{\lambda}_d^2(k) \\ &= -\varepsilon(s_i) y^2(k).\end{aligned} \tag{13}$$

## 3. Stability Analysis

The stability analysis process of closed-loop system (3), (7), and (11) is proposed in this section. First, according to Costa and Fragoso [20], the definition of mean-square stable and the corresponding theorem of decision are shown. The system is

$$x(k+1) = A(\eta(k)) x(k) + B(\eta(k)) \omega(k), \tag{14}$$

where $x(k)$ means the state of the system, $\eta(k)$ means a finite-state, aperiodic, irreducible Markov chain with the value set $S = \{s_1, s_2, \ldots, s_N\}$, $\omega(k)$ means a Gaussian white noise, and $A(\cdot)$ and $B(\cdot)$ mean known positive bounded matrices of appropriate dimensions.

*Definition 1.* System (14) achieves mean-square stability if for every initial value of state $x(0)$ and initial distribution $\eta(0)$, constants $q$ and $Q$ which are independent of $x(0)$ exist and satisfy

$$\begin{aligned} &\left\| \sum_{i=1}^{N} E(x(k) I_{\eta(k)=s_i}) - q \right\| \longrightarrow 0, \quad \text{as } k \longrightarrow \infty, \\ &\left\| \sum_{i=1}^{N} E(x(k) x^T(k) I_{\eta(k)=s_i}) - Q \right\| \longrightarrow 0, \quad \text{as } k \longrightarrow \infty. \end{aligned} \tag{15}$$

**Lemma 1.** *For every given set of symmetric matrices $\{W(s_i) > 0, i = 1, \ldots, N\}$, if a set of symmetric matrices $\{\chi(s_i) > 0, i = 1, \ldots, N\}$ exists and satisfies*

$$\sum_{j=1}^{N} p_{s_i s_j} A^T(s_i) \chi(s_j) A(s_i) - \chi(s_i) = -W(s_i), \tag{16}$$

*then, system (14) is mean-square stable.*

**Theorem 1.** *For every initial value $(y(0), \tilde{\lambda}_d(0))^T$, initial distribution $\sigma(0)$ of the residual gas fraction, and fluctuation of the mass of fresh air $\Delta M_{an}(k)$, closed-loop system (3), (7), and (11) are mean-square stable.*

*Proof.* By (7) and (8), the dynamic of $\tilde{\lambda}_d(k)$ can be described as follows:

$$\tilde{\lambda}_d(k+1) = \tilde{\lambda}_d(k) + c M_{\text{fn}}(k) \tilde{\lambda}_d(k). \tag{17}$$

By rearranging (3), (11), and (17), we have

$$\begin{aligned}\begin{pmatrix} y(k+1) \\ \tilde{\lambda}_d(k+1) \end{pmatrix} &= \begin{pmatrix} 0 & -M_{\text{fn}}(k) \\ 0 & 1 + c M_{\text{fn}}(k) \end{pmatrix} \begin{pmatrix} y(k) \\ \tilde{\lambda}_d(k) \end{pmatrix} \\ &\quad + \begin{pmatrix} \Delta M_{\text{an}}(k) \\ 0 \end{pmatrix}.\end{aligned} \tag{18}$$

Define

$$A(\eta(k)) = \begin{pmatrix} 0 & -M_{\text{fn}}(k) \\ 0 & 1 + cM_{\text{fn}}(k) \end{pmatrix}, \tag{19}$$

and select

$$\chi(\eta(k)) = \begin{pmatrix} \dfrac{1}{\left(\sup\{M_{\text{fn}}(k)\}\right)^2} & 0 \\ 0 & 1 \end{pmatrix}. \tag{20}$$

For each $s_i \varepsilon S$, we get

$$A^T(s_i)\chi(s_j)A(s_i) - \chi(s_i) = -W(s_i), \tag{21}$$

where

$$W(s_i) = \begin{pmatrix} \dfrac{1}{\left(\sup\{M_{\text{fn}}(k)\}\right)^2} & 0 \\ 0 & \dfrac{2M_{\text{fn}}(k)\left(\sup\{M_{\text{fn}}(k)\} - M_{\text{fn}}(k)\right)}{\left(\sup\{M_{\text{fn}}(k)\}\right)^2} \end{pmatrix}. \tag{22}$$

It should be noted that

$$\det\left(\frac{1}{\left(\sup\{M_{\text{fn}}(k)\}\right)^2}\right) > 0, \qquad \det(W(s_i)) > 0, \tag{23}$$

i.e., $W(s_i)$ is a matrix with positive definite and symmetric characteristics. From Lemma 1, closed-loop system (3), (7), and (11) are mean-square stable. □

*Remark 1.* The main results of this work include the design of the adaptive law (5), by which the theoretical air-fuel ratio of biogas-fuelled engines can be estimated online. The design of the stochastic adaptive air-fuel ratio controller (11) for the precision control of the air-fuel ratio considers the uncertainty of the methane concentration in the biogas.

## 4. Numerical Simulation

The proposed stochastic adaptive air-fuel ratio control algorithm (11) is validated by employing the numerical simulation which is similar to [13]:

$$\begin{aligned} y(k) &= M_a(k) - M_f(k)\lambda_d, \\ M_a(k+1) &= \left(M_a(k) - \lambda_d \mu M_f(k)\right) r(k) + M_{\text{an}}(k), \\ M_f(k+1) &= M_f(k)(1-\mu) r(k) + M_{\text{fn}}(k), \\ \dot{M}_{\text{an}} &= \frac{\rho_a V_d \eta_v}{4\pi P_a} \omega_e P_m, \\ T_e &= \frac{H_u V_d \eta_i \eta_v P_m}{4\pi R T_m \lambda}, \\ J\dot{\omega}_e &= T_e - T_l, \\ \dot{P}_m &= \frac{RT_m}{V_m}\left(\dot{M}_i - \dot{M}_{\text{an}}\right), \\ \dot{M}_i &= s_0(1 - \cos\phi)\frac{P_a}{\sqrt{RT_a}}\psi\left(\frac{P_a}{P_m}\right), \end{aligned} \tag{24}$$

where $\dot{M}_{\text{an}}$ means the flow rate of air mass leaving the manifold, $\rho_a$ means the atmospheric density, $V_d$ means the cylinder displacement, $\eta_v$ means the volumetric efficiency, $\omega_e$ means the engine revolution, $P_m$ means the manifold pressure, $P_a$ means the atmospheric pressure, $T_e$ means the mean indicated torque, $H_u$ means the fuel low heating value, $\eta_i$ means the indicated efficiency, $R$ means the constant of gas, $T_m$ means the manifold temperature, $J$ means the rotational inertia, $T_l$ means the external load, $\dot{M}_i$ means the mass flow rate of the air pass throttle, $s_0$ means the area of the throttle, $\phi$ means the opening of the throttle, and

$$\psi(s) = \begin{cases} s^{(2/k)}\left(\dfrac{2k}{k-1}(1-s)\right)^{(k-1/k)}, & \text{if } s \geq \left(\dfrac{2}{k+1}\right)^{(k/k-1)}, \\ k\left(\dfrac{2}{k+1}\right)^{(k+1/k-1)}, & \text{if otherwise.} \end{cases} \tag{25}$$

From (2), $y(k)$ is unmeasured because theoretical air-fuel ratio $\lambda_d$ is undetermined. Therefore, the relationship between $y(k)$ and excess air coefficient $\alpha(k)$ is deduced since $\alpha(k)$ can be measured by the universal exhaust gas oxygen sensor. By the definition of $\alpha(k)$, we have

$$\alpha(k) = \frac{M_a(k)}{\lambda_d M_f(k)}. \tag{26}$$

Using the approximate linearization technology, we obtain

$$\begin{aligned} \alpha(k) &\approx \frac{M_{\text{an}}(k)}{\lambda_d\left(M_{\text{an}}(k)/\lambda_d\right)} + \frac{1}{\lambda_d\left(M_{\text{an}}(k)/\lambda_d\right)}\left(M_a(k) - M_{\text{an}}(k)\right) - \frac{M_{\text{an}}(k)}{\lambda_d\left(M_{\text{an}}^2(k)/\lambda_d^2\right)}\left(M_f(k) - \frac{M_{\text{an}}(k)}{\lambda_d}\right) \\ &= 1 + \frac{M_a(k)}{M_{\text{an}}(k)} - 1 - \frac{\lambda_d M_f(k)}{M_{\text{an}}(k)} + 1 = 1 + \frac{y(k)}{M_{\text{an}}(k)}. \end{aligned} \tag{27}$$

By rearranging (27), we obtain

$$y(k) = (\alpha(k) - 1)M_{\text{an}}(k), \tag{28}$$

where $M_{\text{an}}(k)$ can be measured by the air mass flow rate sensor.

The diagram of the control structure is shown in Figure 1, where $M_{\text{psac}}(k)$ means the proposed stochastic adaptive air-fuel ratio controller and $M_{\text{open}}(k)$ means the open-loop controller which is provided as follows:

$$M_{\text{open}}(k) = \frac{M_{\text{an}}(k)}{\lambda_{d,m}}, \tag{29}$$

where $\lambda_{d,m}$ denotes the theoretical air-fuel ratio which is measured by the methane concentration sensor.

Numerical simulation is run in case 1 and case 2, and each case has two working conditions. Under working condition W11 of case 1, the theoretical air-fuel ratio is an unknown constant, the engine revolution is 1200 rpm, and the external load is 60 Nm. Under working condition W12 of case 1, the theoretical air-fuel ratio is also an unknown constant, the engine revolution is 1600 rpm, and the external load is 90 Nm. The signals of the excess air coefficient of $M_{\text{psac}}(k)$ and $M_{\text{open}}(k)$ under W11 and W12 are shown in Figure 2. In Figure 2, the excess air coefficient can be regulated into a neighbourhood of 1. Figure 3 exhibits the adaptive law and the measured theoretical air-fuel ratio under W11 and W12. In Figure 3, the adaptive law of each working condition is adjusted to a steady value, while the measured theoretical air-fuel ratio fluctuates due to the application of the methane concentration sensor.

The control performance indices of $M_{\text{psac}}(k)$ and $M_{\text{open}}(k)$ over 20,000 sampling points under W11 and W12 of case 1 are provided in Table 1, where

$$J(N) = \sum_{k=1}^{N} (\alpha(k) - 1)^2. \tag{30}$$

Table 1 shows that the dispersion of the excess air coefficient of $M_{\text{psac}}(k)$ is narrower than that of $M_{\text{open}}(k)$, which indicates that $M_{\text{psac}}(k)$ has better control performance under every working condition.

In case 2, the theoretical air-fuel ratio is the jump signal of each working condition. In working condition W21 of case 2, the engine revolution is 1200 rpm, and the external load is 60 Nm. In working condition W22, the engine revolution is 1600 rpm, and the external load is 90 Nm. Figure 4 shows the excess air coefficient of $M_{\text{psac}}(k)$ and $M_{\text{open}}(k)$ under W21 and W22, where both controllers are effective when the theoretical air-fuel ratio is the jump signal. The adaptive law and measured theoretical air-fuel ratio under W21 and W22 of case 2 are

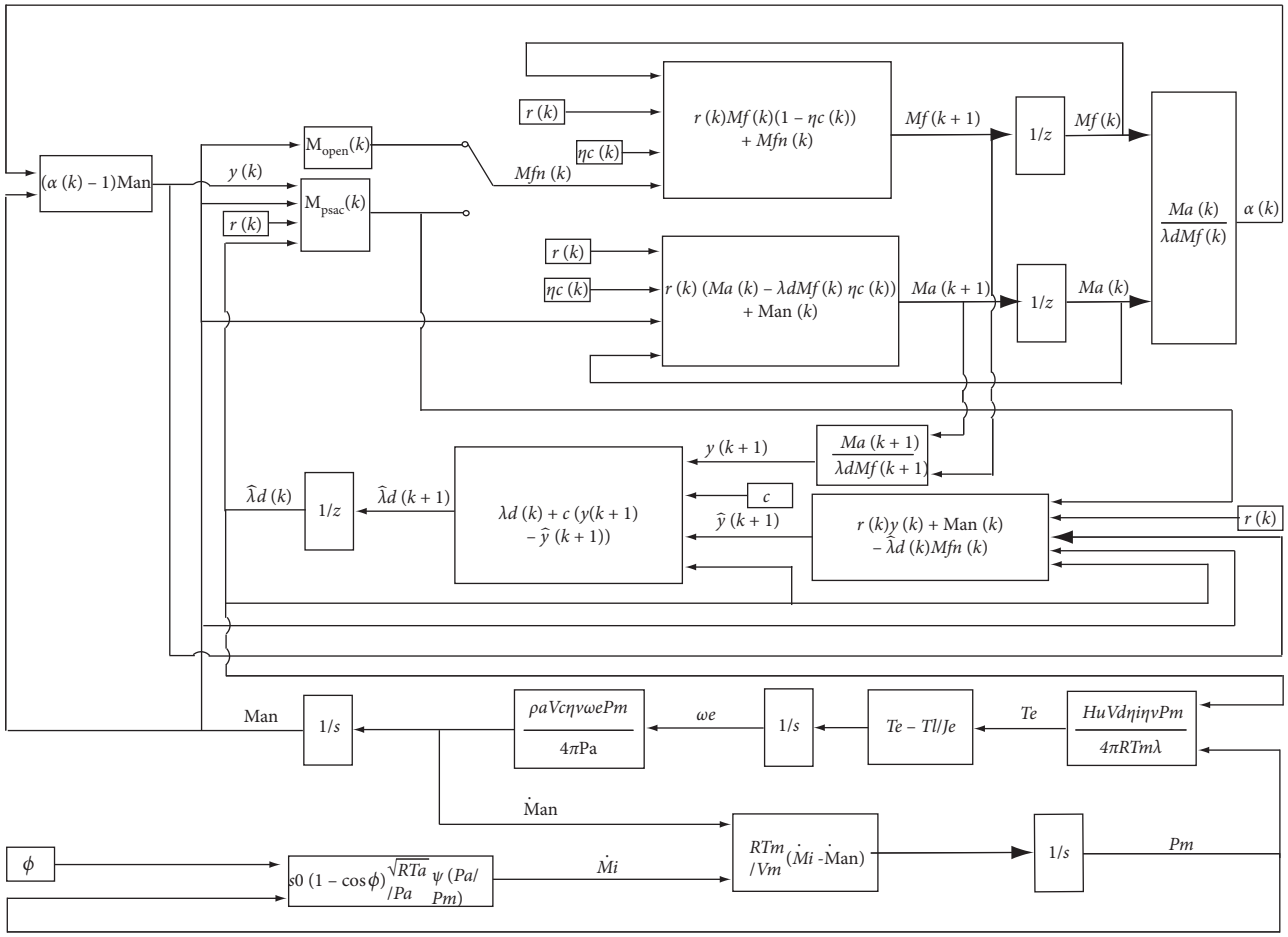


Figure 1: Diagram of the control structure.

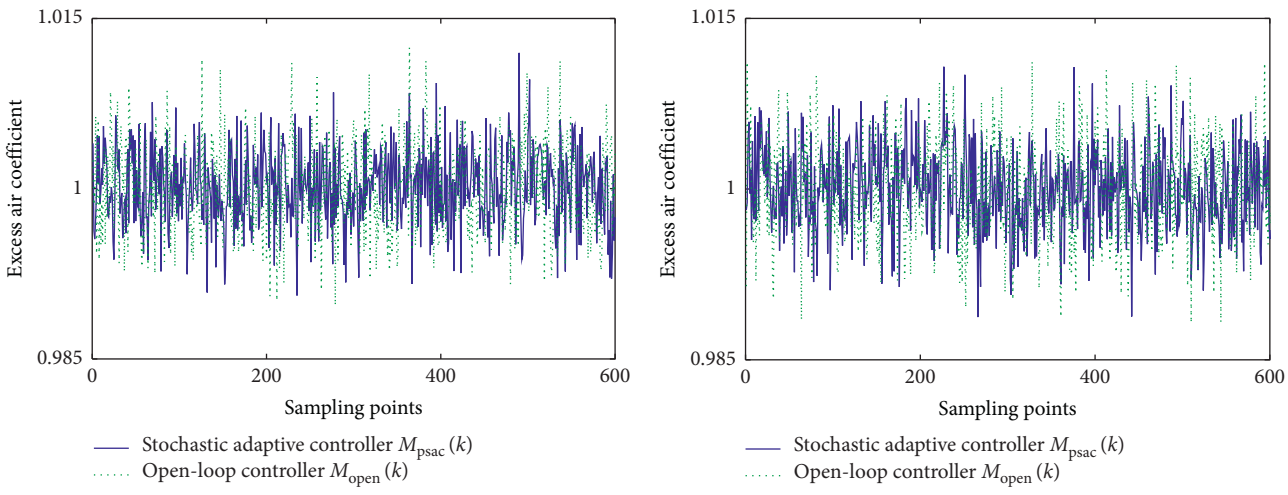


Figure 2: Excess air coefficient of case 1. (a) W11. (b) W12.

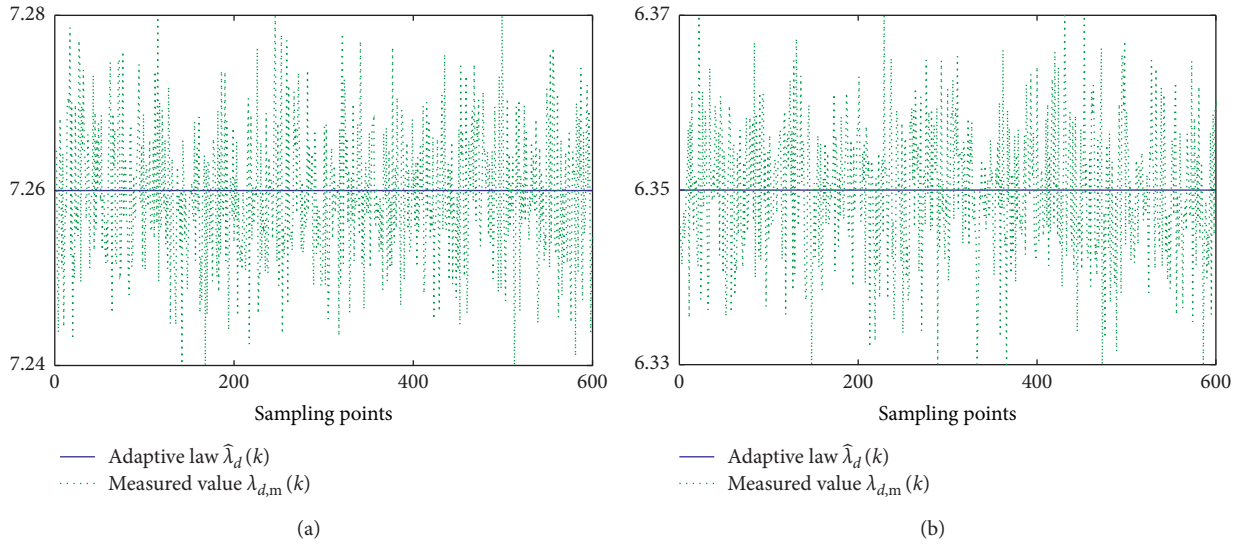


Figure 3: Adaptive law and measured theoretical air-fuel ratio of case 1. (a) W11. (b) W12.

Table 1: Control performance indices under W11 and W12 of case 1.

| | W11 | W12 |
|---|---|---|
| $J_{M_{\mathrm{psac}}(k)}(20000)$ | 0.5019 | 0.6286 |
| $J_{M_{\mathrm{open}}(k)}(20000)$ | 0.5552 | 0.6981 |

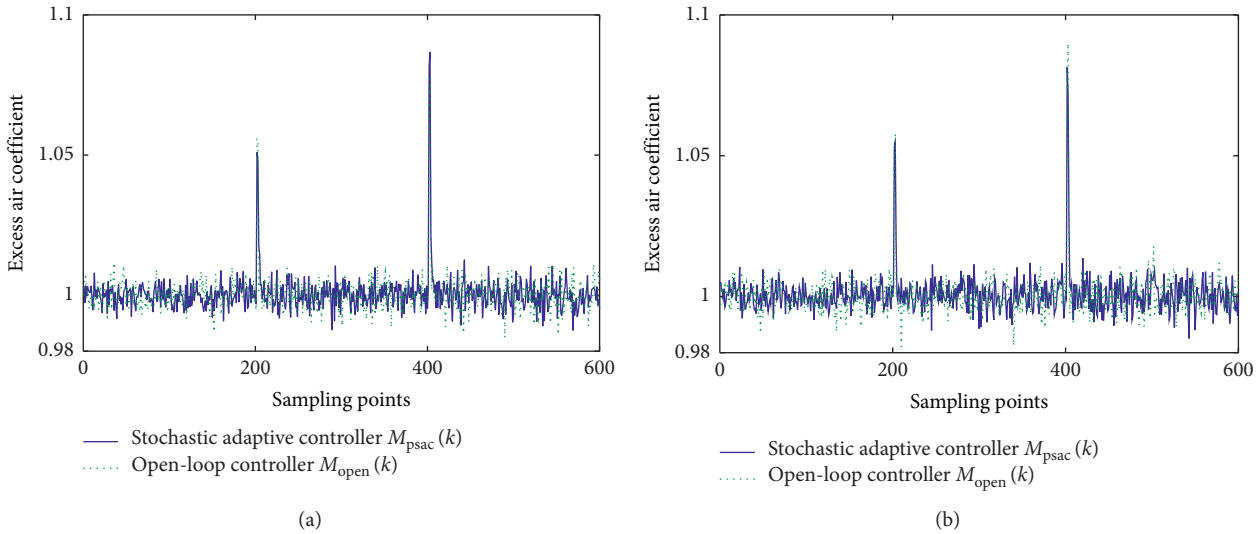


Figure 4: Excess air coefficient of case 2. (a) W21. (b) W22.

provided in Figure 5. Figure 5 shows that the theoretical air-fuel ratio can be estimated by the adaptive law when it is a jumped signal, and the measured value of the theoretical air-fuel ratio of each working condition fluctuates because of the application of the methane concentration sensor.

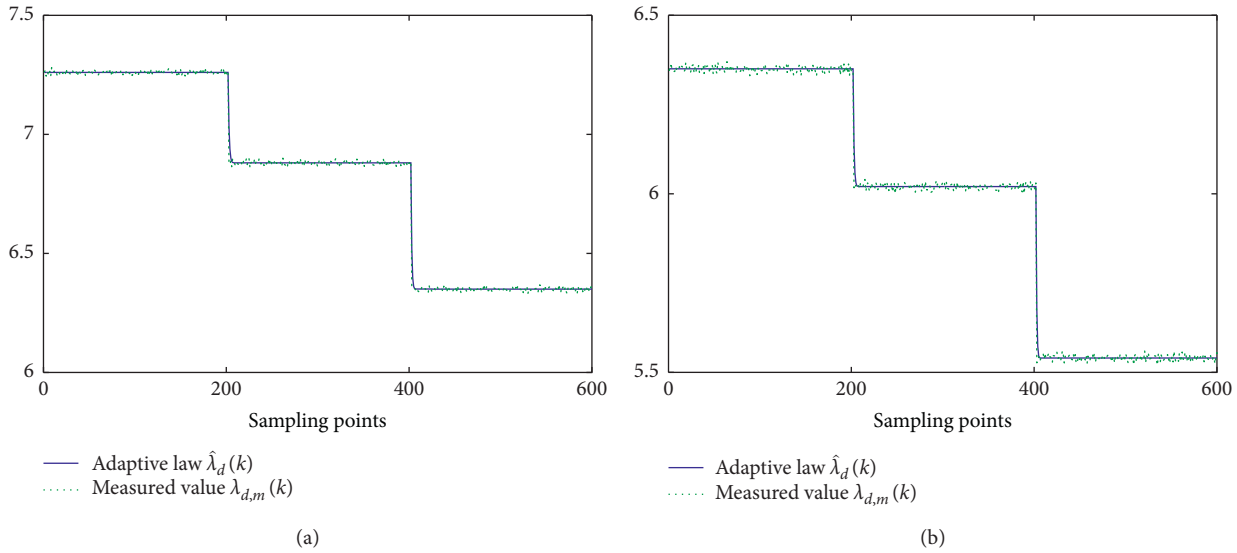


Figure 5: Adaptive law and measured theoretical air-fuel ratio of case 2. (a) W21. (b) W22.

## 5. Conclusions

In this paper, the stochastic adaptive air-fuel ratio controller has been designed for the engines fuelled by biogas since the uncertainty of the methane concentration in biogas greatly affects the control accuracy of the air-fuel ratio. The closed-loop system, which consists of the dynamic model of the regulation error of the air-fuel ratio, proposed stochastic adaptive air-fuel ratio controller, and adaptive law, has been proven to be mean-square stable. The control performance of the proposed stochastic adaptive air-fuel ratio controller has been compared to that of the open-loop controller in two cases through a numerical simulation. The simulation results show that the proposed stochastic adaptive air-fuel ratio controller achieves better control performance. In future work, the control performance of other alternative fuels such as methanol will be researched.

## Data Availability

No data were used to support this study.

## Conflicts of Interest

The authors declare that there are no conflicts of interest regarding the publication of this paper.

## Acknowledgments

This work was supported by the National Natural Science Foundation of China (Grant no. 61803231), Shandong Provincial Higher School Youth Innovation Technology Project of China (Grant no. 2020KJB002), and Shandong Provincial Research and Development Project of China (Grant no. 2019GSF111049).

## References

[1] S. Y. Ragadia and R. C. Iyer, "A review paper on theoretical & experimental investigations of a biogas engine technology," *International Journal for Scientific Research and Development*, vol. 3, pp. 864–869, 2015.

[2] B. V. Ga and T. V. Nam, "Appropriate structural parameters of biogas SI engine converted from diesel engine," *IET Renewable Power Generation*, vol. 9, no. 3, pp. 255–261, 2015.

[3] K. A. Rahman and A. Ramesh, "Effect of reducing the methane concentration on the combustion and performance of a biogas diesel predominantly premixed charge compression ignition engine," *Fuel*, vol. 206, pp. 117–132, 2017.

[4] S. Verma, L. M. Das, and S. C. Kaushik, "Effects of varying composition of biogas on performance and emission characteristics of compression ignition engine using exergy analysis," *Energy Conversion and Management*, vol. 138, pp. 346–359, 2017.

[5] I. T. Yilmaz and M. Gumus, "Investigation of the effect of biogas on combustion and emissions of TBC diesel engine," *Fuel*, vol. 188, pp. 69–78, 2017.

[6] K. A. Rahman and A. Ramesh, "Studies on the effects of methane fraction and injection strategies in a biogas diesel common rail dual fuel engine," *Fuel*, vol. 236, pp. 147–165, 2019.

[7] G. Tripathi, P. Sharma, and A. Dhar, "Effect of methane augmentations on engine performance and emissions," *Alexandria Engineering Journal*, vol. 59, no. 1, pp. 429–439, 2020.

[8] S. Y. Ragadia, C. L. Rajesh, and A. Dhar, "Experimental investigations on the influence of compression ratio and piston crown geometry on the performance of biogas fuelled small spark ignition engine," *Renewable Energy*, vol. 146, pp. 997–1009, 2020.

[9] L. Ma, N. Xu, X. Huo et al., "Adaptive finite-time output-feedback control design for switched pure-feedback nonlinear systems with average dwell time," *Nonlinear Analysis: Hybrid Systems*, vol. 37, pp. 1–23, 2020.

[10] Y. Chang, Y. Wang, F. E. Alsaadi, and G. Zong, "Adaptive fuzzy output–feedback tracking control for switched stochastic pure–feedback nonlinear systems," *International Journal of Adaptive Control and Signal Processing*, vol. 33, no. 10, pp. 1567–1582, 2019.

[11] L. Ma, X. Huo, X. Zhao, and G. Zong, "Adaptive fuzzy tracking control for a class of uncertain switched nonlinear

systems with multiple constraints: a small-gain approach," *International Journal of Fuzzy Systems*, vol. 21, no. 8, pp. 2609–2624, 2019.

[12] B. Wu, X. H. Chang, and X. D. Zhao, "Fuzzy $H_\infty$ output feedback control for nonlinear NCSs with quantization and stochastic communication protocol," *IEEE Transactions on Fuzzy Systems, Early Access*, 2020, In press.

[13] S. Xie, X. Hu, Z. Xin, and L. Li, "Time-efficient stochastic model predictive energy management for a plug-in hybrid electric bus with an adaptive reference state-of-charge advisory," *IEEE Transactions on Vehicular Technology*, vol. 67, no. 7, pp. 5671–5682, 2018.

[14] H. Kazemi, H. N. Mahjoub, A. Tahmasbi-Sarvestani, and Y. P. Fallah, "A learning-based stochastic MPC design for cooperative adaptive cruise control to handle interfering vehicles," *IEEE Transactions on Intelligent Vehicles*, vol. 3, no. 3, pp. 266–275, 2018.

[15] D. Selmanaj, G. Panzani, S. van Dooren, J. Rosgren, and C. Onder, "Adaptive and unconventional strategies for engine knock control," *IEEE Transactions on Control Systems Technology*, vol. 27, no. 4, pp. 1838–1845, 2019.

[16] Z. Pu, X. Jiao, C. Yang, and S. Fang, "An adaptive stochastic model predictive control strategy for plug-in hybrid electric bus during vehicle-following scenario," *IEEE Access*, vol. 8, pp. 13887–13897, 2020.

[17] X.-H. Chang, Y. Liu, and M. Shen, "Resilient control design for lateral motion regulation of intelligent vehicle," *IEEE/ASME Transactions on Mechatronics*, vol. 24, no. 6, pp. 2488–2497, 2019.

[18] J. Yang, T. L. Shen, and X. H. Jiao, "Model-based stochastic optimal air-fuel ratio control with residual gas fraction of spark ignition engines," *IEEE Transactions on Control Systems Technology*, vol. 22, pp. 895–910, 2014.

[19] P.-C. Yeh and P. V. Kokotović, "Adaptive control of a class of nonlinear discrete-time systems," *International Journal of Control*, vol. 62, no. 2, pp. 303–324, 1995.

[20] O. L. V. Costa and M. D. Fragoso, "Stability results for discrete-time linear systems with markovian jumping parameters," *Journal of Mathematical Analysis and Applications*, vol. 179, no. 1, pp. 154–178, 1993.